Stress distribution pattern in all-on-four maxillary restorations supported by porous tantalum and solid titanium implants using three-dimensional finite element analysis

Faeze Masoomi, Farhang Mahboub

Department of Prosthodontic, Faculty of Dentistry, Tabriz University of Medical Sciences, Tabriz, Iran.

Abstract

Success/failure of dental implants depends on stress transfer and distribution at the bone-implant interface. This study aimed to assess the stress distribution pattern in all-on-four maxillary restorations supported by porous tantalum and solid titanium implants using three-dimensional (3D) finite element analysis (FEA). In this FEA, a geometric model of an edentulous maxilla, Zimmer screw-vent tantalum and solid titanium implants were modelled. Four models with the all-on-four concept were designed. The fifth model had 6 vertical implants (all-on-six). Two different implant types (porous tantalum and solid titanium) were modelled to yield a total of 10 models, and subjected to 200 N bilateral vertical load. Pattern of stress distribution and maximum von Mises stress values in cancellous and cortical bones around implants were analysed. In tantalum models, the effect of increasing the distal tilting of posterior implants was comparable to the effect of increasing the number of implants to 6 on von Mises stress values in cortical bone. However, in cancellous bone, the effect of increasing the tilting of posterior implants on stress was slightly greater than the effect of increasing the number of implants to 6. In solid titanium models, the effect of both of the abovementioned parameters was comparable on stress in cancellous bone; but in cortical bone, the effect of increasing the implant number was slightly greater on stress reduction. Despite similar pattern of stress distribution in bone around implants, higher maximum von Mises stress values around tantalum implants indicate higher stress transfer capacity of this type of implant to the adjacent bone, compared with solid titanium implants.

Key Words: finite element analysis; dental implants; maxilla; tantalum.

Eur J Transl Myol 34 (1) 12170, 2023 doi: 10.4081/ejtm.2024.12170

Adequate bone quality and quantity is an important prerequisite for dental implant placement. Patients with severe alveolar bone loss primarily require bone augmentation procedures.[1] The anatomical properties of an edentulous maxilla complicate the reconstruction of atrophic ridge with dental implants. Several invasive approaches have been proposed for augmentation of severely atrophic maxilla such as bone grafting and sinus floor augmentation, aiming to augment the bone.[2-4] Thus, the all-on-four concept was first introduced for mandible in 2003 and for maxilla in 2005; to maximize benefitting from the residual bone in an atrophic jaw.[5,6] This protocol includes placement of four dental implants in the anterior part of a completely edentulous ridge (two anterior implants placed axially and two posterior implants placed with up to 45degree distal tilting) to support a fixed temporary restoration for immediate loading.[7,8] Accordingly, placement of posterior implants parallel to the anterior sinus wall, along with a distal tilt,[7,9,10] improves skeletal anchorage and support,[10,11] decreases the length of cantilever, and results in more favorable stress distribution in bone.[9,12-16] However, the amount of stress generated in bone supporting the tilted implants remains questionable, and FEA showed controversial results regarding the magnitude of stress in the cervical bone and implant neck in distally tilted implants.[17,18] The success of implant treatment depends on a number of factors such as implant characteristics (design, material, and fabrication process), and pattern of stress distribution in implant and its supporting structures. Implant design characteristics affect stress distribution and transfer from the implant to the surrounding bone, and play a role in its long-term success/failure as such.[19] Therefore, qualitative and quantitative assessment of stress distribution in dental implants and the supporting bone is imperative to predict the behavior of implants in the oral

environment.[20] Porous tantalum implants have been extensively used in medicine and dental implants in the past 15 years and their clinical success has been well documented.[21,22] In this particular type of dental implants, the term "osseoincorporation" is preferably used instead of osseointegration for providing of biologic anchorage, which is defined as a combination of bone-implant contact and ingrowth of bone into the porous tantalum.[23] Porous implants have two favorable properties contributing to their extensive use.[24] The first one is their elastic modulus which is similar to the elastic modulus of bone, and prevents stress isolation at the bone interfaceand preserves the mineral density of the peri-implant bone.[24,25] Another advantage is its structural properties that allow bone ingrowth to achieve biologic fixation.[26,27] Accordingly, in addition to osseointegration, bone penetrates into a geometric network of inter-connected pores and further increases the implant anchorage.[28-30] The combination of osseointegration and osseoincorporation results in significantly increased secondary stability of dental implants in bone.[25] Also, the high frictional effects increase the primary stability of porous tantalum implants in bone.[31,32] Theoretically, porous tantalum implants can serve as a valuable strategy for treatment of patients with type III and IV bone. Increased surface area provided by the tantalum (TM) shell can result in faster and more firm osseointegration.[23] FEA is extensively used for quantitative assessment of stress distribution in implants and the supporting bone.[20,33] Due to the high complexity of the geometry of the implant-bone system, FEA is the most suitable tool for assessment of this system.[34] Considering the advantages of all-on-four implant-supported restorations in edentulous patients, and the challenges related to the success of titanium implant treatment in patients with poor quality bone, use of porous tantalum implants has gained increasing attention. Thus, this study aimed to compare stress distribution pattern in all-on-four maxillary restorations supported by porous tantalum and solid titanium implants using three-dimensional (3D) FEA. The null hypothesis was that the pattern of load distribution would not be significantly different in all-on-six (conventional method), and all-on-four (with 0, 15, 30, and 45-degree tilting of distal implants) restorations supported by solid titanium and porous tantalum implants under 200 N vertical load.

Materials and Methods

Designing of the models

Three-dimensional geometry of an edentulous maxilla, including the cortical and cancellous bones, was designed by using computed tomography scans of an edentulous patient with no maxillofacial anomaly and normal craniofacial ratios with Mimics software. The maxillary arch had an approximate radius of 25 mm, with 140 mm length, 18 mm height, and 9 mm width. To simulate type III bone, one layer of cortical bone with 1 mm thickness was designed covering the entire maxilla while

cancellous bone was used for the central parts of the alveolus.[35] For implant modeling, two screw-vent trabecular tantalum implants with 11.5 and 13 mm lengths and 4.1 mm diameter, and two screw-vent solid titanium implants with 11.5 and 13 mm lengths and 4.1 mm diameter were used. The trabecular part of the porous tantalum implants was designed in the form of a layer with 0.75 mm thickness and 4.5 mm height such that it started at 2 mm from the implant end. Similar to the cancellous bone, this layer was considered isotropic and homogenous. Considering the fabrication process of Zimmer trabecular metal TM, which is chemical vapor infiltration-chemical vapor deposition, the modulus of elasticity of the porous tantalum layer was considered to be averagely 3000 MPa.[36] The 3D geometric data of the edentulous maxilla and dental implants were assessed by ATOS II optical digitizing system, and the obtained data were transferred to ABAQUS modelling and processing software. Next, the implants along with the abutment and suprastructure were virtually placed in bone. To design an all-on-four model, two mesial implants were placed vertically and bilaterally at the site of lateral incisors, and two distal implants were placed at the site of first premolars with 0, 15, 30, and 45-degree distal tilts [37]. Two cylindrical titanium abutments with straight profile were modeled and placed on vertical implants while two abutments with 15, 30, and 45-degree angulations were
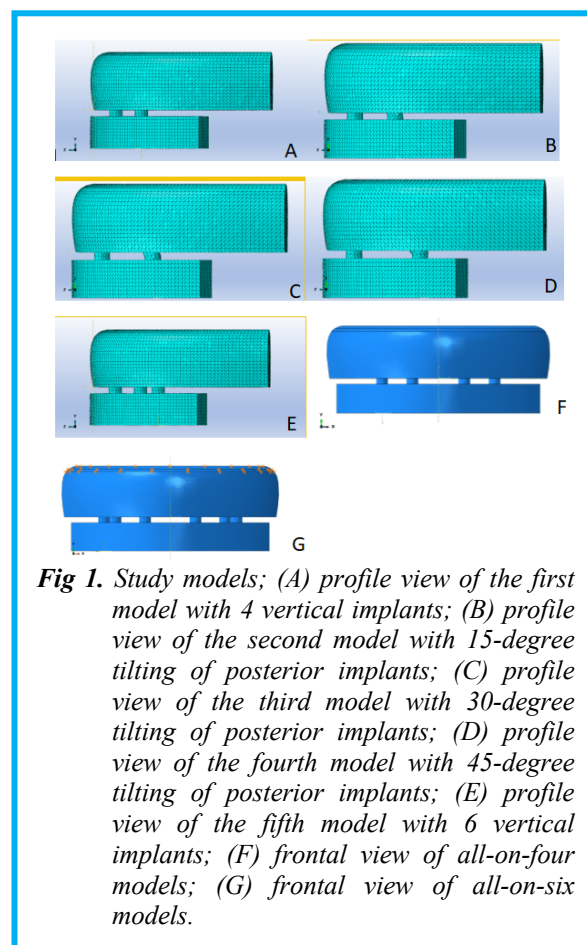

Fig 1. *Study models; (A) profile view of the first model with 4 vertical implants; (B) profile view of the second model with 15-degree tilting of posterior implants; (C) profile view of the third model with 30-degree tilting of posterior implants; (D) profile view of the fourth model with 45-degree tilting of posterior implants; (E) profile view of the fifth model with 6 vertical implants; (F) frontal view of all-on-four models; (G) frontal view of all-on-six models.*

Table 1. *Total number of elements and nodes in different models.*

Titanium models	Elements	Nodes
All-on-four (0-degree)	261078	49960
All-on-four (15-degree)	263246	50252
All-on-four (30-degree)	274833	52029
All-on-four (45-degree)	264978	50370
All-on-six	282431	53177
Tantalum models	Elements	Nodes
All-on-four (0-degree)	261319	48737
All-on-four (15-degree)	255798	45329
All-on-four (30-degree)	268435	51361
All-on-four (45-degree)	261808	50144
All-on-six	285038	53371

placed on tilted implants.[35] The titanium suprastructure was designed by the modeling software in the form of a prosthetic bar with height and buccolingual width of 10 mm, and peripheral length of 93 mm (which included the mesiodistal width of 12 masticatory units).[37] In total, four models of all-on-four full-arch maxillary prostheses and one all-on-six model were designed for each of the two implant designs (porous and solid).[37] In the first model, 4 vertical implants were bilaterally placed at the site of lateral incisors and first premolars according to the protocol by Zarb et al.[38] In the second to fourth models, the anterior implants were vertical and the posterior implants had a distal tilt (by 15, 30, and 45 degrees, respectively). In the fifth model, six vertical implants (conventional method) were virtually placed at the site of lateral incisors and first and second premolars bilaterally. The implant height in all models was 11.5 mm, except for posterior implants in the third and fourth models, which

had 13 mm height, due to greater distal tilt and to ensure that the apex of posterior implants would be placed along the longitudinal axis of the first premolar. Although the length of suprastructure was the same in all models, the length of distal cantilevers varied (20, 16, 12, and 9.5 mm in the first to fourth models, respectively, and 13 mm in the fifth model).[37] Figure 1 shows the models. After designing of the models, they were processed in ABAQUS software, and meshed using 3D tetrahedral four-node elements. The total number of elements and nodes in different models is presented in Table 1.

Material properties
Table 2 presents the material properties including the elasticity coefficient and Poisson's ratio [25, 35, 36, 39, 40]. All materials were considered isotropic, homogenous, and linearly elastic.[35,36,39]

Boundary conditions and interfaces
The boundary conditions of the models were defined according to the uniformity of the maxilla and base of skull, such that the movement of the maxilla was restricted, and these conditions were applied to the upper part of bone. All peripheral nodes of the model were fixed and their movement was completely restricted.[35,39] The bone-implant interface was modeled with complete osseointegration with completely fixed tie attachment. There was no gap at the implant-abutment connection, and the attachment was modeled as completely fixed.[35,39] The attachment of suprastructure-abutment was also considered as tie for the screw-retained restoration.[37] Perfect sit situation was considered between the implants, bone, and prosthetic suprastructure.[35,39]

Loading conditions
Each of the five models for the two implant designs was subjected to 200 N static load bilaterally, simultaneously, and vertically, which was applied to the first molar region (right and left cantilevers).[35,39] The maximum von Mises stress and its distribution in the surrounding bone (cortical and cancellous) were assessed in each model. The results of mathematical solutions were converted to visual results depicted by color degrees in the range of red and blue, such that red color indicated higher level of stress and blue color indicated lower level of stress.

Table 2. *Material properties.*

Material	Young's modulus (GPa)	Poisson's ratio	References
Porous Tantalum (CVI/CVP)	3 (2/5-3/5)	0.3	25,36
Ti-6Al-4V	103.4	0.35	36
Cortical bone	13.7	0.30	35,36,39,40
Trabecula bone (type III)	1.37	0.30	35,36,39,40

***Table 3.** Maximum von Mises stress.*

Maximum von Mises stress (MPa) values	Cortical bone	Cancellous bone	Difference (cortical bone)	Difference (cancellous bone)
M01 (First model)	76.2	10.04	29.2 higher	4.41 higher
M02 (Second model)	43.76	9.23	3.11 higher	4.03 higher
M03 (Third model)	36.2	6.17	1 higher	1.34 higher
M04 (Fourth model)	35.8	4.48	< 1 higher	0.17 lower
M05 (Fifth model)	36.6	6.56	5.2 higher	1.8 higher
M06 (Sixth model)	47	5.63	29.2 lower	4.41 lower
M07 (Seventh model)	40.65	5.2	3.11 lower	4.03 lower
M08 (Eighth model)	35.15	4.83	1 lower	1.34 lower
M09 (Ninth model)	34.9	4.65	< 1 lower	0.17 higher
M10 (Tenth model)	31.4	4.75	5.2 lower	1.8 lower

Results

Table 3 presents the maximum von Mises stress values in the surrounding bone (cortical and cancellous) of each model and the differences between corresponding models of tantalum trabecular and titanium solid implants.

M01 (First model)

Full-arch titanium bar was supported by 4 screw-vent tantalum trabecular vertical implants with 20-mm bilateral cantilevers (Fig. 2A).
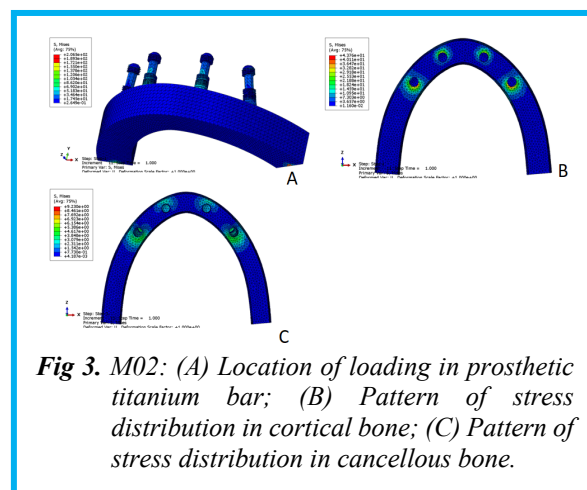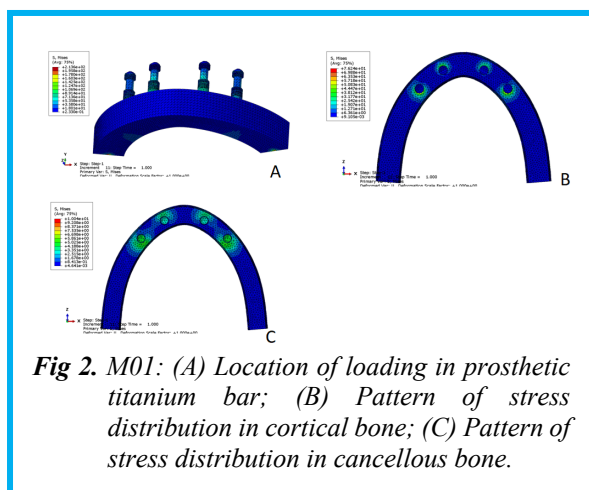
Stress distribution in cortical and cancellous bones

The maximum von Mises stresses in this model, in both cortical and cancellous bones were the highest among all models (Table 3, respectively 76.2 and 10.4 MPa) (Fig. 2B and Fig. 2C).

M02 (Second model)

Full-arch titanium bar was supported by 4 screw-vent tantalum trabecular implants with 16-mm bilateral cantilevers and posterior implants with 15-degree distal tilt (Fig. 3A). Stress distribution in cortical and cancellous bones The maximum von Mises stresses in this model, in cortical and cancellous bones were respectively 42.5% and 8% lower than the first model. Also, greater stress distribution towards the distal was noted compared with the M01 model (Table 3, Fig. 3B and Fig. 3C).
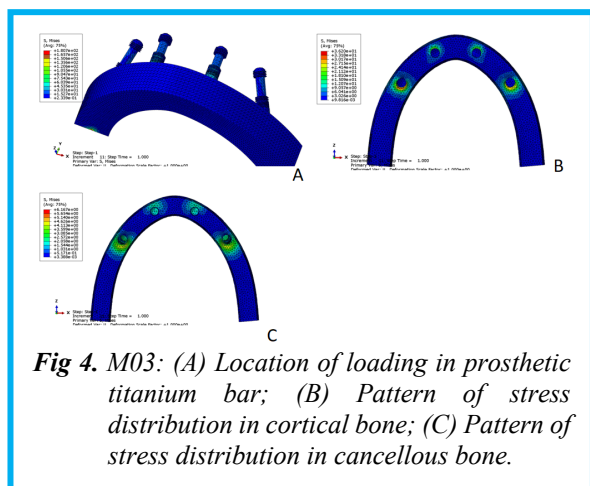

***Fig 2.** M01: (A) Location of loading in prosthetic titanium bar; (B) Pattern of stress distribution in cortical bone; (C) Pattern of stress distribution in cancellous bone.*

***Fig 3.** M02: (A) Location of loading in prosthetic titanium bar; (B) Pattern of stress distribution in cortical bone; (C) Pattern of stress distribution in cancellous bone.*

Fig 4. *M03: (A) Location of loading in prosthetic titanium bar; (B) Pattern of stress distribution in cortical bone; (C) Pattern of stress distribution in cancellous bone.*

Fig 5. *M04: (A) Location of loading in prosthetic titanium bar; (B) Pattern of stress distribution in cortical bone; (C) Pattern of stress distribution in cancellous bone.*

M03 (Third model)

Full-arch titanium bar was supported by 4 screw-vent tantalum trabecular implants with 12-mm bilateral cantilevers and posterior implants with 30-degree distal tilt (Fig. 4A).

Stress distribution in cortical and cancellous bones

The stress distribution was more distal along the crest compared with the first and second models. The maximum von Mises stresses in this model, in cortical and cancellous bones were respectively 52.5% and 38.5% lower than the M01 model (Table 3, Fig. 4B and Fig. 4C).

M04 (Fourth model)

Full-arch titanium bar was supported by 4 screw-vent tantalum trabecular implants with 9.5-mm bilateral cantilevers and posterior implants with 45-degree distal tilt (Fig. 5A).

Stress distribution in cortical and cancellous bones

The pattern of stress distribution was more distal along the crest compared with the abovementioned models. The maximum von Mises stresses in this model, in cortical and cancellous bones were respectively 53% (the lowest amongst tantalum models and almost similar to the value in the M03 model) and 55% (the lowest amongst all
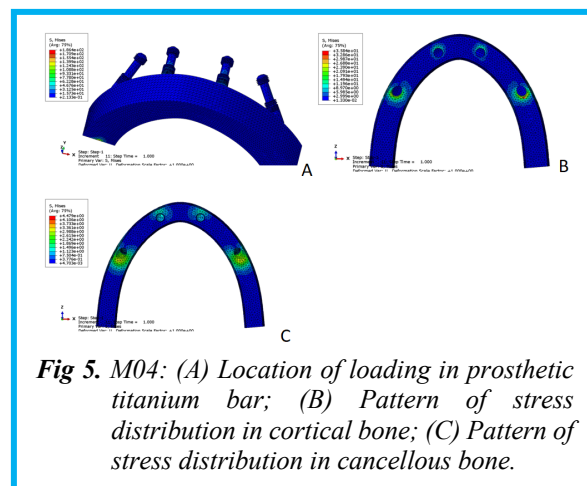
models) lower than the M01 model (Table 3, Fig. 5B and Fig. 5C).

M05 (Fifth model)

Full-arch titanium bar was supported by 6 vertical screw-vent tantalum trabecular implants with 13-mm bilateral cantilevers (Fig. 6A).

Stress distribution in cortical and cancellous bones

The pattern of stress distribution had less extension towards the distal compared with the M02 to M04 models. The maximum von Mises stresses in this model, in cortical and cancellous bones were respectively 52% (similar to the M03 and M04 models) and 34.6% lower than that in the M01 model. The stress in bone around the two anterior implants was higher than that around middle implants, and lower than that in posterior implants. The lowest stress was noted around middle implants (Table 3, Fig. 6B and Fig. 6C).

M06 (Sixth model)

Full-arch titanium bar was supported by 4 vertical tapered screw-vent solid titanium implants with 20-mm bilateral cantilevers (Fig. 7A).

Stress distribution in cortical and cancellous bones

The maximum von Mises stresses in this model, in both cortical and cancellous bones were the highest among
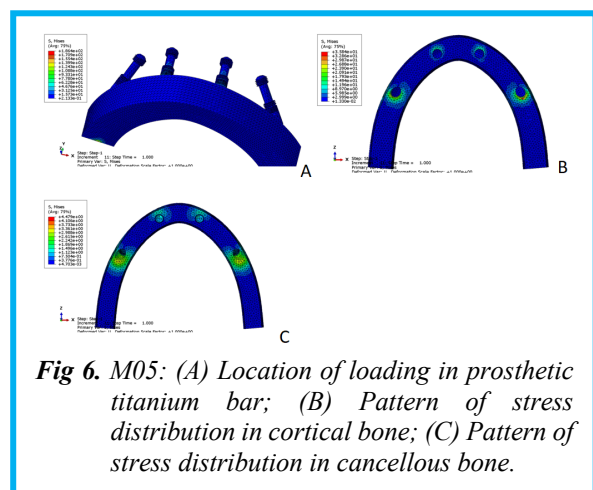

Fig 6. *M05: (A) Location of loading in prosthetic titanium bar; (B) Pattern of stress distribution in cortical bone; (C) Pattern of stress distribution in cancellous bone.*
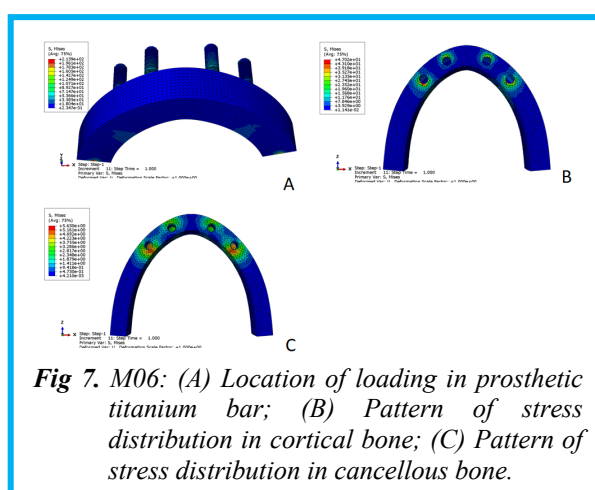

Fig 7. *M06: (A) Location of loading in prosthetic titanium bar; (B) Pattern of stress distribution in cortical bone; (C) Pattern of stress distribution in cancellous bone.*
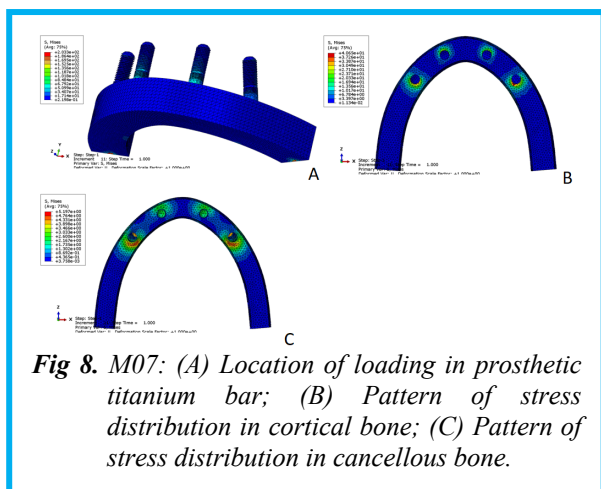
Fig 8. *M07: (A) Location of loading in prosthetic titanium bar; (B) Pattern of stress distribution in cortical bone; (C) Pattern of stress distribution in cancellous bone.*

Fig 9. *M08: (A) Location of loading in prosthetic titanium bar; (B) Pattern of stress distribution in cortical bone; (C) Pattern of stress distribution in cancellous bone.*
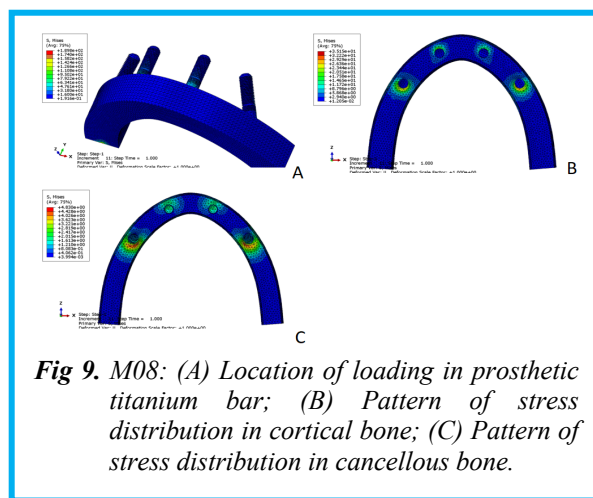
titanium models (Table 3, respectively 47 and 5.63 MPa) (Fig. 7B and Fig. 7C).

M07 (Seventh model)

Full-arch titanium bar was supported by 4 tapered screw-vent solid titanium implants with 16-mm bilateral cantilevers and 15-degree distal tilting of posterior implants (Fig. 8A).

Stress distribution in cortical and cancellous bones

The maximum von Mises stresses in this model, in cortical and cancellous bones were respectively 13.5% and 7.6% lower than that in the M06 model. In cortical bone, stress pattern had a slightly greater distal distribution and in cancellous bone, the pattern of distribution towards the distal was similar to that in the

M08 (Eighth model)

Full-arch titanium bar was supported by 4 tapered screw-vent solid titanium implants with 12-mm bilateral cantilevers and 30-degree distal tilting of posterior implants (Fig. 9A).

Stress distribution in cortical and cancellous bones

The pattern of stress distribution was more distally than the previous two models. The maximum von Mises

stresses in this model, in cortical and cancellous bones were respectively 25.2% and 14.2% lower than that in the M06 model (Table 3, Fig. 9B and Fig. 9C).

M09 (Ninth model)

Full-arch titanium bar was supported by 4 tapered screw-vent solid titanium implants with 9.5-mm bilateral cantilevers and 45-degree distal tilting of posterior implants (Fig. 10A).

Stress distribution in cortical and cancellous bones

The pattern of stress distribution was more distally than the previous models. The maximum von Mises stresses in this model, in cortical and cancellous bones were respectively 25.7% (almost similar to the M08 model) and 17.4% (the lowest amongst solid titanium models) lower than that in the M06 model (Table 3, Fig. 10B and Fig. 10C).

M10 (Tenth model)

Full-arch titanium bar was supported by 6 vertical tapered screw-vent solid titanium implants with 13-mm bilateral cantilevers (Fig. 11A).

Stress distribution in cortical and cancellous bones
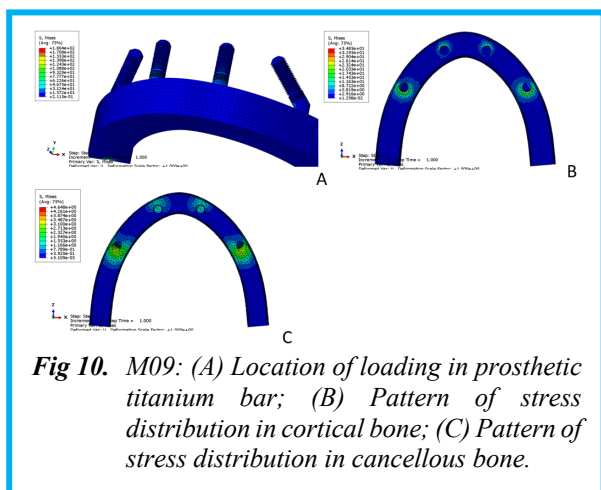
Compared with the M06 to M09 models, stresses not only

Fig 10. *M09: (A) Location of loading in prosthetic titanium bar; (B) Pattern of stress distribution in cortical bone; (C) Pattern of stress distribution in cancellous bone.*

Fig 11. *M10: (A) Location of loading in prosthetic titanium bar; (B) Pattern of stress distribution in cortical bone; (C) Pattern of stress distribution in cancellous bone.*
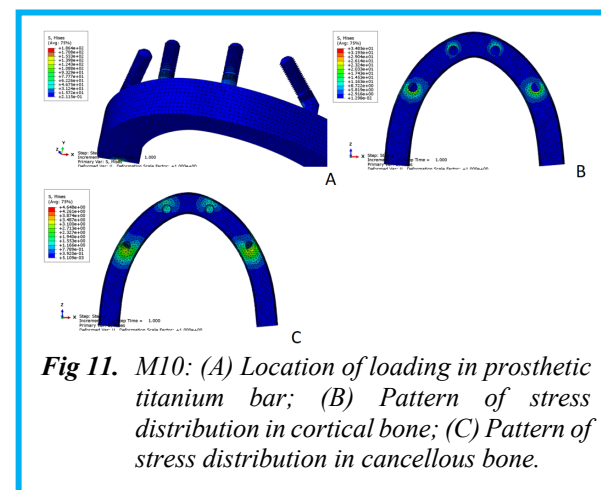
affected the distal of bone surrounding posterior implants, but also the mesial of bone, and all the crestal area was involved. Thus, stresses were spread all around the posterior implants. The maximum von Mises stresses in this model, in cortical and cancellous bones were respectively 33.2% (the lowest amongst all models and maximum reduction compared with previous models) and 15.6% lower than that in the M06 model. Stresses around the two anterior implants were higher than middle implants and lower than posterior implants. Middle implants had the lowest stress (Table 3, Fig. 11B and Fig. 11C).

Overall comparison of the results of different all-on-four and all-on-six models supported by screw-vent tantalum trabecular and tapered screw-vent solid titanium implants

In all of the models, in both cortical and cancellous bones, maximum stress accumulation was noted in the crestal bone around posterior implants, especially in the distal region. Stress values in bone around anterior implants were low, compared with posterior implants, and the stresses were mainly concentrated anterior to implants. By advancing towards the apical part of implants, the amount of stress decreased and they had a wider distribution. In both cortical and cancellous bones, by an increase in tilting of posterior implants, the maximum von Mises stress decreased; however, stress distributed in a more extensive area and extended towards the distal along the crestal bone. Anterior implants in all-on-four models and middle implants in all-on-six models experienced the minimum amount of stress. In both cortical and cancellous bones around tantalum implants, the maximum von Mises stress was higher than that in the corresponding models with solid titanium implants, such that in the M01 model, the highest stress was recorded in both cortical and cancellous bones. Although this difference between titanium and tantalum implants was greater in more vertical all-on-four models and gradually decreases by an increase in tilting of posterior implants or implant number in all-on-six models, thus the stress values approximate each other.

Discussion

This study compared stress distribution pattern in all-on-four maxillary restorations supported by porous tantalum and solid titanium implants using 3D FEA. The null hypothesis was that the pattern of load distribution would not be significantly different in all-on-six (conventional method), and all-on-four (with 0, 15, 30, and 45-degree tilting of distal implants) models supported by solid titanium and porous tantalum implants under 200 N load. According to the obtained results, the null hypothesis of the study was accepted. Similar to previous studies [16,37], the present results revealed that in all models, the stress value in cortical bone was higher than that in cancellous bone, which can be attributed to the higher elasticity coefficient of cortical bone, creating higher

stress values. Saleh Saber et al. [37] found that as the angulation of posterior implants increased in all-on-four models and extended towards the distal along the crestal bone, stress at the level of cervical part of posterior implants decreased in both cortical and cancellous bones. In other words, more vertical posterior implants and greater length of cantilever result in higher and more concentrated pattern of von Mises stress. The present results confirmed their findings in both solid titanium and porous tantalum implants. They compared all-on-four model with 45-degree tilting of posterior implants with all-on-six model, and reported almost similar stress values in cortical bone. However, the stress value in cancellous bone was lower in 45-degree tilting model. They concluded that using two more implants with longer cantilever would not decrease stress in cancellous bone. Thus, it appears that the cantilever length is the primary factor, and can decrease stress even in presence of smaller number of implants. However, in the present study, in solid titanium implant models (in cancellous bone), increasing the tilt of posterior implants and subsequent reduction in cantilever length had no significant difference with increasing the number of implants to 6 with respect to the reduction of stress values, and both were found to be important factors that can decrease the level of stress. The present results in tantalum implants were closer to their findings, and the stress value in cortical bone was almost the same in all-on-four model with 45-degree tilt and all-on-six model. But, in cancellous bone, the 45-degree model showed lower stress level. Difference between the present results and their findings regarding solid titanium models can be due to the fact that the cantilever length in 45-degree model in their study was the lowest amongst all models (2.5 mm), and its negative effect on stress was largely decreased. However, in the present study, the cantilever length in 45-degree model was 9.5 mm, which was considerable and could still exert negative effects under 200 N cantilever loading. Evidence shows that the occlusal force on posterior teeth is approximately 220 N.[41,42] The pattern of loading in the present study was similar to that in a study by Gianpaolo;[35] however, they reported that stress concentration in 45-degree model was almost twice the value in 15- and 30-degree models, which was different from the present results. The cantilever length of the three models was equal in their study (3.5 mm). Stress value in their study was highly affected by implant tilting. They recommended lower degree of implant tilting, a short cantilever, or higher number of implants for optimal stress distribution at the bone-implant interface in clinical cases with biomechanical risk factors such as bruxism or poor quality of bone.

According to the present results and some other studies,[17,43] increasing the tilt of posterior implants in all-on-four models can result in better load distribution and lower stress level, if allows increasing the inter-implant distance and lower cantilever length.

Consistent with the results of Bhering et al.,[44] similar mechanical behavior of both all-on-six and all-on-four concepts may be related to their similar clinical success in full-arch fixed four- or six-implant-supported restorations. Although Bhering et al.[44] concluded that all-on-six was the most favorable concept regarding biomechanical behavior and lower stress compared with all-on-four, it should be noted that in this study, the all-on-four group had a 6.69 mm cantilever and the all-on-six group had no cantilever; this factor, along with the higher number of posterior implants, results in lower stress and more favorable biomechanical behavior.

Although several studies have reported an increase in stress by increasing the length of cantilever, a FEA by van Zyl et al.[45] defined an optimum range < 15 mm, and reported that exceeding 15 mm length can cause greater stresses in buccal and lingual cortical plates and compromise the integrity of bone. This statement may explain more favorable stress distribution and lower stress values by increasing the distal tilting of implants (30 and 45 degrees) with < 15 mm cantilever length in all-on-four and all-on-six models.

In the present study, despite the same stress distribution patterns, the von Mises stress values were higher in tantalum than solid titanium implants. Similarly, Sertgöz reported that materials with lower modulus of elasticity did not show significant differences in stress distribution patterns in peri-implant bone while stiffer materials tended to absorb some of the stress, which is referred to as stress isolation.[46] Such materials, due to higher modulus of elasticity, further absorb the stress and transfer less stress to the other parts including the adjacent bone.[42] This can explain higher level of stress in bone around tantalum implants in the present study since tantalum has lower modulus of elasticity than titanium (close to that of bone) and transfers greater stress to the bone. The effect of framework material on stress distribution in all-on-four and all-on-six models should not be overlooked either.[42] Future studies should address the effect of framework material on stress distribution in all-on-four and all-on-six concepts.

This study had some limitations. FEA results should be interpreted with caution since FEA cannot fully simulate the clinical setting.[47] Moreover, future studies should consider anisotropic, viscous, non-linear, and non-homogenous bone properties that can respond to stress in the form of resorption or regeneration under muscular and external time-dependent loads. Also, longitudinal clinical follow-ups and randomized clinical trials are required to verify the present findings in the clinical setting.[44,48] Finally, future studies should assess the effect of cyclic loading with different angulations.

In conclusion, despite similar pattern of stress distribution in bone around porous tantalum and solid titanium implants, higher maximum von Mises stress values around tantalum implants indicate higher stress transfer capacity of this type of implant to the adjacent bone, compared with solid titanium implants.

List of acronyms

3D - three-dimensional
FEA - finite element analysis

Contributions of Authors

The authors designed the models and performed the simulations. Faeze M reviewed the results and made comparison between the models and wrote the manuscript. Farhang M conceived the study, supervised it and revised the manuscript. All authors read and approved the final edited manuscript.

Conflict of Interest

The authors declare no conflict(s) of interest related to the publication of this study.

Ethical Publication Statement

We confirm that we have read the Journal's position on issues involved in ethical publication and affirm that this report is consistent with those guidelines.

Corresponding Author

Farhang Mahboub, Department of Prosthodontic, Faculty of Dentistry, Tabriz University of Medical Sciences, Tabriz, Iran.
ORCID iD: 0000-0003-2113-8028
 E-mail: farhangmahboub92@gmail.com

E-mails and ORCID iD of co-authors

Faeze Masoomi: faezeh.dds.94@gmail.com
ORCID iD: 0000-0002-8869-8823

References

1. Asawa N, Bulbule N, Kakade D, Shah R. Angulated implants: an alternative to bone augmentation and sinus lift procedure: systematic review. J Clin Diagn Res. 2015 Mar;9(3):ZE10-3.doi: 10.7860/JCDR/2015/11368.5655. Epub 2015 Mar 1. PMID: 25954718; PMCID: PMC4413168.

2. Esposito M, Hirsch JM, Lekholm U, Thomsen P. Biological factors contributing to failures of osseointegrated oral implants. (I). Success criteria and epidemiology. Eur J Oral Sci. 1998 Feb;106(1):527-51. doi: 10.1046/j.0909-8836..t01-2-.x. PMID: 9527353.

3. Cricchio G, Lundgren S. Donor site morbidity in two different approaches to anterior iliac crest bone harvesting. Clin Implant Dent Relat Res. 2003;5(3):161-9. doi: 10.1111/j.1708-8208.2003.tb00198.x. PMID: 14575632.

4. Nkenke E, Schultze-Mosgau S, Radespiel-Tröger M, Kloss F, Neukam FW. Morbidity of harvesting of chin grafts: a prospective study. Clin Oral Implants Res. 2001 Oct;12(5):495-502. doi: 10.1034/j.1600-0501.2001.120510.x. PMID: 11564110..

5 Maló P, Rangert B, Dvärsäter L. Immediate function of Brånemark implants in the esthetic zone: a retrospective clinical study with 6 months to 4 years of follow-up. Clin Implant Dent Relat Res. 2000;2(3):138-46. doi: 10.1111/j.1708-8208.2000.tb00004.x. PMID: 11359258..

6. Durkan R, Oyar P, Deste G. Maxillary and mandibular all-on-four implant designs: A review. Niger J Clin Pract. 2019 Aug;22(8):1033-1040. doi: 10.4103/njcp.njcp_273_18. PMID: 31417044.

7. Maló P, Rangert B, Nobre M. All-on-4 immediate-function concept with Brånemark System implants for completely edentulous maxillae: a 1-year retrospective clinical study. Clin Implant Dent Relat Res. 2005;7 Suppl 1:S88-94. doi: 10.1111/j.1708-8208.2005.tb00080.x. PMID: 16137093.

8. Takahashi T, Shimamura I, Sakurai K. Influence of number and inclination angle of implants on stress distribution in mandibular cortical bone with All-on-4 Concept. J Prosthodont Res. 2010 Oct;54(4):179-84. doi: 10.1016/j.jpor.2010.04.004. Epub 2010 May 10. PMID: 20452854.

9. Aparicio C, Perales P, Rangert B. Tilted implants as an alternative to maxillary sinus grafting: a clinical, radiologic, and periotest study. Clin Implant Dent Relat Res. 2001;3(1):39-49. doi: 10.1111/j.1708-8208.2001.tb00127.x. PMID: 11441542.

10. Krekmanov L, Kahn M, Rangert B, Lindström H. Tilting of posterior mandibular and maxillary implants for improved prosthesis support. Int J Oral Maxillofac Implants. 2000 May-Jun;15(3):405-14. PMID: 10874806.

11. Skalak R. Biomechanical considerations in osseointegrated prostheses. J Prosthet Dent. 1983 Jun;49(6):843-8. doi: 10.1016/0022-3913(83)90361-x. PMID: 6576140.

12. Krekmanov L. Placement of posterior mandibular and maxillary implants in patients with severe bone deficiency: a clinical report of procedure. Int J Oral Maxillofac Implants. 2000 Sep-Oct;15(5):722-30. PMID: 11055139.

13. Calandriello R, Tomatis M. Simplified treatment of the atrophic posterior maxilla via immediate/early function and tilted implants: A prospective 1-year clinical study. Clin Implant Dent Relat Res. 2005;7 Suppl 1:S1-12. doi: 10.1111/j.1708-8208.2005.tb00069.x. PMID: 16137082.

14. Mattsson T, Köndell PA, Gynther GW, Fredholm U, Bolin A. Implant treatment without bone grafting in severely resorbed edentulous maxillae. J Oral Maxillofac Surg. 1999 Mar;57(3):281-7. doi: 10.1016/s0278-2391(99)90673-0. PMID: 10077198.

15. Aparicio C. A retrospective clinical and radiographic evaluation of tilted implants used in the treatment of the severely resorbed edentulous maxilla. Appl Osseointegration Res 2002; 3:17-21.

16. Bevilacqua M, Tealdo T, Menini M, Pera F, Mossolov A, Drago C, Pera P. The influence of cantilever length and implant inclination on stress distribution in maxillary implant-supported fixed dentures. J Prosthet Dent. 2011 Jan;105(1):5-13. doi: 10.1016/S0022-3913(10)60182-5. PMID: 21194582..

17. Zampelis A, Rangert B, Heijl L. Tilting of splinted implants for improved prosthodontic support: a two-dimensional finite element analysis. J Prosthet Dent. 2007 Jun;97(6 Suppl):S35-43. doi: 10.1016/S0022-3913(07)60006-7. Erratum in: J Prosthet Dent. 2008 Mar;99(3):167. PMID: 17618932.

18. Cağlar A, Aydin C, Ozen J, Yilmaz C, Korkmaz T. Effects of mesiodistal inclination of implants on stress distribution in implant-supported fixed prostheses. Int J Oral Maxillofac Implants. 2006 Jan-Feb;21(1):36-44. PMID: 16519180.

19. Bahrami B, Shahrbaf S, Mirzakouchaki B, Ghalichi F, Ashtiani M, Martin N. Effect of surface treatment on stress distribution in immediately loaded dental implants--a 3D finite element analysis. Dent Mater. 2014 Apr;30(4):e89-97. doi: 10.1016/j.dental.2014.01.012. Epub 2014 Feb 18. PMID: 24559526.

20. Sahin S, Cehreli MC, Yalçin E. The influence of functional forces on the biomechanics of implant-supported prostheses--a review. J Dent. 2002 Sep-Nov;30(7-8):271-82. doi: 10.1016/s0300-5712(02)00065-9. PMID: 12554107.

21. Shimko DA, Shimko VF, Sander EA, Dickson KF, Nauman EA. Effect of porosity on the fluid flow characteristics and mechanical properties of tantalum scaffolds. J Biomed Mater Res B Appl Biomater. 2005 May;73(2):315-24. doi: 10.1002/jbm.b.30229. PMID: 15736288.

22. Meneghini RM, Ford KS, McCollough CH, Hanssen AD, Lewallen DG. Bone remodeling around porous metal cementless acetabular components. J Arthroplasty. 2010 Aug;25(5):741-7. doi: 10.1016/j.arth.2009.04.025. Epub 2009 May 26. PMID: 19473807.

23. Bencharit S, Byrd WC, Altarawneh S, Hosseini B, Leong A, Reside G, Morelli T, Offenbacher S. Development and applications of porous tantalum trabecular metal-enhanced titanium dental implants. Clin Implant Dent Relat Res. 2014 Dec;16(6):817-26. doi: 10.1111/cid.12059. Epub 2013 Mar 25. PMID: 23527899; PMCID: PMC3708989.

24. Chen LJ. Finite Element Analysis of the Stress on the Implant-Bone Interface of Dental Implants with

Different Structures. Finite Element Analysis – New Trends and Developments. 2012; Chapter 3:55-72.

25. Liu Y, Bao C, Wismeijer D, Wu G. The physicochemical/biological properties of porous tantalum and the potential surface modification techniques to improve its clinical application in dental implantology. Mater Sci Eng C Mater Biol Appl. 2015 Apr;49:323-329. doi: 10.1016/j.msec.2015.01.007. Epub 2015 Jan 6. PMID: 25686956.

26. Vaillancourt H, Pilliar RM, McCammond D. Factors affecting crestal bone loss with dental implants partially covered with a porous coating: a finite element analysis. Int J Oral Maxillofac Implants. 1996 May-Jun;11(3):351-9. PMID: 8752556.

27. Pilliar RM, Deporter DA, Watson PA, Valiquette N. Dental implant design--effect on bone remodeling. J Biomed Mater Res. 1991 Apr;25(4):467-83. doi: 10.1002/jbm.820250405. PMID: 2050711.

28. Unger AS, Lewis RJ, Gruen T. Evaluation of a porous tantalum uncemented acetabular cup in revision total hip arthroplasty: clinical and radiological results of 60 hips. J Arthroplasty. 2005 Dec;20(8):1002-9. doi: 10.1016/j.arth.2005.01.023. PMID: 16376255..

29. Wigfield C, Robertson J, Gill S, Nelson R. Clinical experience with porous tantalum cervical interbody implants in a prospective randomized controlled trial. Br J Neurosurg. 2003 Oct;17(5):418-25. doi: 10.1080/02688690310001611206. PMID: 14635746..

30. Tsao AK, Roberson JR, Christie MJ, Dore DD, Heck DA, Robertson DD, Poggie RA. Biomechanical and clinical evaluations of a porous tantalum implant for the treatment of early-stage osteonecrosis. J Bone Joint Surg Am. 2005;87 Suppl 2:22-7. doi: 10.2106/JBJS.E.00490. PMID: 16326720.

31. Romanos GE, Delgado-Ruiz RA, Sacks D, Calvo-Guirado JL. Influence of the implant diameter and bone quality on the primary stability of porous tantalum trabecular metal dental implants: an in vitro biomechanical study. Clin Oral Implants Res. 2018 Jun;29(6):649-655. doi: 10.1111/clr.12792. Epub 2016 Feb 24. PMID: 26916451.

32. Kim DG, Huja SS, Tee BC, Larsen PE, Kennedy KS, Chien HH, Lee JW, Wen HB. Bone ingrowth and initial stability of titanium and porous tantalum dental implants: a pilot canine study. Implant Dent. 2013 Aug;22(4):399-405. doi: 10.1097/ID.0b013e31829b17b5. PMID: 23823737.

33. Sato Y, Wadamoto M, Tsuga K, Teixeira ER. The effectiveness of element downsizing on a three-dimensional finite element model of bone trabeculae in implant biomechanics. J Oral Rehabil.

1999 Apr;26(4):288-91. doi: 10.1046/j.1365-2842.1999.00390.x. PMID: 10232856.

34. Geng JP, Tan KB, Liu GR. Application of finite element analysis in implant dentistry: a review of the literature. J Prosthet Dent. 2001 Jun;85(6):585-98. doi: 10.1067/mpr.2001.115251. PMID: 11404759.

35. Sannino G. All-on-4 concept: a 3-dimensional finite element analysis. J Oral Implantol. 2015 Apr;41(2):163-71. doi: 10.1563/AAID-JOI-D-12-00312. Epub 2013 Apr 5. PMID: 23560570.

36. Akbarzadeh A, Hemmati Y, Saleh-Saber F. Evaluation of stress distribution of porous tantalum and solid titanium implant-assisted overdenture in the mandible: A finite element study. Dent Res J (Isfahan). 2021 Dec 10;18:108. PMID: 35265291; PMCID: PMC8804542.

37. Saleh Saber F, Ghasemi S, Koodaryan R, Babaloo A, Abolfazli N. The Comparison of Stress Distribution with Different Implant Numbers and Inclination Angles In All-on-four and Conventional Methods in Maxilla: A Finite Element Analysis. J Dent Res Dent Clin Dent Prospects. 2015 Fall;9(4):246-53. doi: 10.15171/joddd.2015.044. Epub 2015 Dec 30. PMID: 26889362; PMCID: PMC4753034.

38. Zarb GA, editor. Osseointegration: on continuing synergies in surgery, prosthodontics, biomaterials. Quintessence Publishing Company; 2008. p. 23-5.

39. Kumari A, Malhotra P, Phogat S, Yadav B, Yadav J, Phukela SS. A finite element analysis to study the stress distribution on distal implants in an all-on-four situation in atrophic maxilla as affected by the tilt of the implants and varying cantilever lengths. J Indian Prosthodont Soc. 2020 Oct-Dec;20(4):409-416. doi: 10.4103/jips.jips_70_20. Epub 2020 Oct 8. PMID: 33487969; PMCID: PMC7814689.

40. Sevimay M, Turhan F, Kiliçarslan MA, Eskitascioglu G. Three-dimensional finite element analysis of the effect of different bone quality on stress distribution in an implant-supported crown. J Prosthet Dent. 2005 Mar;93(3):227-34. doi: 10.1016/j.prosdent.2004.12.019. PMID: 15775923.

41. Horita S, Sugiura T, Yamamoto K, Murakami K, Imai Y, Kirita T. Biomechanical analysis of immediately loaded implants according to the "All-on-Four" concept. J Prosthodont Res 2017; 61:123-32.

42. Kelkar KC, Bhat V, Hegde C. Finite element analysis of the effect of framework materials at the bone-implant interface in the all-on-four implant system. Dent Res J (Isfahan). 2021 Feb 23;18:1. PMID: 34084288; PMCID: PMC8122683.

43. Bellini CM, Romeo D, Galbusera F, Agliardi E, Pietrabissa R, Zampelis A, Francetti L. A finite element analysis of tilted versus nontilted implant configurations in the edentulous maxilla. Int J

Prosthodont. 2009 Mar-Apr;22(2):155-7. PMID: 19418861.

44. Bhering CL, Mesquita MF, Kemmoku DT, Noritomi PY, Consani RL, Barão VA. Comparison between all-on-four and all-on-six treatment concepts and framework material on stress distribution in atrophic maxilla: A prototyping guided 3D-FEA study. Mater Sci Eng C Mater Biol Appl. 2016 Dec 1;69:715-25. doi: 10.1016/j.msec.2016.07.059. Epub 2016 Jul 21. PMID: 27612765.

45 van Zyl PP, Grundling NL, Jooste CH, Terblanche E. Three-dimensional finite element model of a human mandible incorporating six osseointegrated implants for stress analysis of mandibular cantilever prostheses. Int J Oral Maxillofac Implants. 1995 Jan-Feb;10(1):51-7. PMID: 7615317.

46. Sertgöz A. Finite element analysis study of the effect of superstructure material on stress distribution in an implant-supported fixed prosthesis. Int J Prosthodont. 1997 Jan-Feb;10(1):19-27. PMID: 9484066.

47. Lewis MB, Klineberg I. Prosthodontic considerations designed to optimize outcomes for single-tooth implants. A review of the literature. Aust Dent J. 2011 Jun;56(2):181-92. doi: 10.1111/j.1834-7819.2011.01322.x. PMID: 21623811..

48. Baggi L, Pastore S, Di Girolamo M, Vairo G. Implant-bone load transfer mechanisms in complete-arch prostheses supported by four implants: a three-dimensional finite element approach. J Prosthet Dent. 2013 Jan;109(1):9-21. doi: 10.1016/S0022-3913(13)60004-9. PMID: 23328192.

Disclaimer